

White light source with laser-excited phosphor

O.R. Abdullaev, A.V. Aluev, Yu.L. Akhmerov, N.V. Kourova,
M.V. Mezhenyi, A.A. Chelny

Abstract. The principles of operation of a white light source based on a remote phosphor, made of cerium-doped yttrium aluminium garnet (YAG:Ce³⁺), whose luminescence is excited by a blue laser diode, are considered. The colorimetric and photometric characteristics of phosphors of different types are analysed as functions of the phosphor film thickness. The following parameters are obtained at an output power of 1 W and a wavelength of 445±3 nm in the cw regime: luminous flux of 165 lm, correlated colour temperature of 5595 K, colour rendering index of 66, colour coordinates $x = 0.3303$ and $y = 0.3427$, luminous efficiency of 165 lm W⁻¹, and light efficacy of 30 lm W⁻¹. These characteristics are comparable with similar parameters of commercial white LEDs.

Keywords: semiconductor laser, laser diode, fibre-optic module, phosphor, luminescence, photoluminescence.

1. Introduction

The market volume of lighting systems based on white LEDs constantly increases, with gradual replacement of conventional light sources (incandescent and luminescence lamps). The light sources based on white LEDs are applied in car industry; household, architectural, commercial, and decorative illumination systems; and medicine (stomatology and ophthalmology). As compared with conventional light sources, white LEDs have a number of significant advantages: small size, low consumption of electric energy, long lifetime (up to 50000 h), and high light efficacy.

The operation principle of a white LED is based on the photoluminescence effect. The light emitted by a blue LED passes through a phosphor layer incorporated in a transparent compound. Powder of cerium-doped yttrium aluminium garnet (YAG:Ce³⁺) is used as a phosphor. A mixture of phosphors can be applied to improve the photometric characteristics. When passing through the phosphor layer, some part of the light emitted by the blue LED is absorbed in this layer to excite its yellow luminescence, whereas the rest of the blue light passes without absorption. On the whole, the output light is perceived by human eye as white; it is characterised by colour coordinates x and y , accepted by the Commission internationale de l'éclairage in 1931 (CIE 1931); correlated colour temperature (CCT); and colour rendering index (CRI) [1].

O.R. Abdullaev, A.V. Aluev, Yu.L. Akhmerov, N.V. Kourova,
M.V. Mezhenyi, A.A. Chelny JSC 'Optron', ul. Shcherbakovskaya
53, 105187 Moscow, Russia; e-mail: yuri.akhmerov@yandex.ru

Received 4 April 2017; revision received 28 June 2017
Kvantovaya Elektronika 47 (10) 927–931 (2017)
Translated by Yu.P. Sin'kov

Blue LEDs are fabricated from heterostructures based on nitride compounds of the III group. They contain multi-quantum wells (MQWs) in the active region. Despite all its advantages, a blue LED has a number of fundamental drawbacks as a semiconductor device, which limit the maximum output power per emitter (LED chip).

(i) The spontaneous radiation, arising due to the recombination of electron–hole pairs, propagates in all directions. Because of the total internal reflection, most of this radiation remains in the crystal [1], as a result of which the external quantum efficiency decreases.

(ii) At high carrier injection levels (exceeding current density of 15–17 A cm⁻²), one observes a decrease in the internal quantum efficiency (an effect referred to as the efficiency drop). It is explained by a number of reasons: carrier leakage [2, 3], Auger recombination [4], heating of the active region [5], inhomogeneous active-region composition [6, 7], or a combination of these factors.

In contrast to blue LEDs, blue laser diodes are free of these drawbacks. Laser radiation, propagating in waveguide layers, is incident almost normally on the laser crystal–air interface; therefore, the total internal reflection does not affect the external quantum efficiency and almost all generated light can be extracted into environment with low internal loss. In addition, because of the very high recombination rate, the carrier concentration in the laser active region barely changes with an increase in the pump current when the threshold conditions are reached; therefore, the internal quantum efficiency remains constant even at current densities multiply exceeding the threshold value.

Thus, laser diodes can be considered as promising semiconductor radiation sources for exciting phosphor luminescence in radically new illuminating devices; their potential is confirmed, in particular, by the constant rise in the number of publications in this subject area [8–15]. The application of blue laser diodes in photometric devices may ensure the volume of their commercial production comparable with that of laser diodes for recording–reading information systems (CD-R/CD-RW, DVD-R/DVD-RW, Blu-ray Disc – BD).

In this study, we analyse the possibility of applying classical technology of fabrication of phosphor coatings in order to replace blue LEDs with blue laser diodes in illumination systems.

2. Experimental

The laser radiation source was a NDB7875 laser diode (Nichia), emitting at a wavelength of $\lambda = 445 \pm 3$ nm in the cw regime. A fibre-optic module with a silica fibre (core and shell diameters 105 and 125 μm , respectively; NA = 0.22) was

designed based on this source. The coupling ratio of the laser beam into the fibre was 84%. The colorimetric and photometric characteristics were measured in the cw regime at the fibre-optic module output power $P_{\text{out}} = 1$ W.

Samples of $\text{YAG}:\text{Ce}^{3+}$ powder from different Russian manufacturers were used as phosphors. A phosphor sample was inserted in a transparent organic silicon compound. The ratio of the phosphor and compound mass fractions was maintained constant. A phosphor–compound mixture was deposited on the surface of a flask made of an optically transparent material; we prepared samples of phosphor films with different thicknesses, which were coated by a protective layer of organic silicon compound.

Figure 1a shows an optical scheme of the device. The distal end face of the silica fibre in the module is equipped with a FC-PC connector, which is connected with a transition flange. An optically transparent flask is mounted in the flange. Film samples were deposited on the flask surface. The transition flange was made so that the laser beam divergence angle at the optical fibre output was not limited. A photograph of a white light source with an output power $P_{\text{out}} = 1$ W in the cw regime is shown in Fig. 1b.

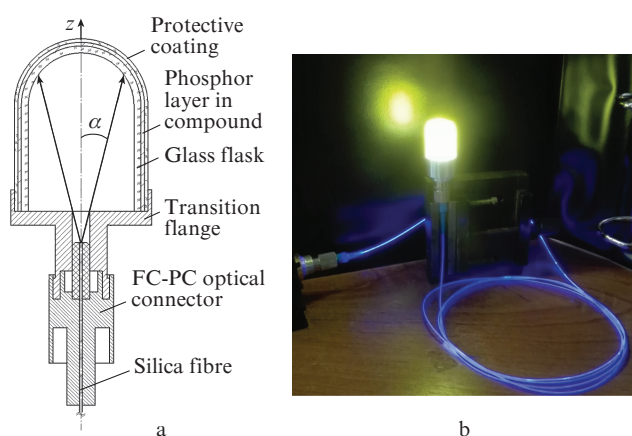


Figure 1. (a) Optical scheme of a white light source based on laser excitation of phosphor and (b) a photograph of this source with an output power $P_{\text{out}} = 1$ W, operating in the cw regime.

Table 1 contains data on the phosphor, its manufacturer, average grain size, and phosphor coating thickness.

The output power of the fibre-optic module was measured using a PM-100 meter (ThorLabs). The spectral characteristics, colour coordinates x and y , CCT, and CRI were recorded

Table 1. Main parameters of phosphor coating films.

Sample	Phosphor type	Manufacturer	Average grain size/ μm	Layer thickness h/mm
1				0.6
2	FLZh-7-560	Luminophor R&PC	10	1.0
3				1.4
4				0.6
5	SDL-4000	Platan R&DI with a pilot plant	20	1.0
6				1.4
7				0.6
8	SDL-3500	Platan R&DI with a pilot plant	20	1.0
9				1.4

by an MK-350 meter (UPRTec). The luminous flux F_v was measured using a TKA-KK1 integrating sphere.

3. Results and discussion

Table 2 contains measured values of colour coordinates and photometric characteristics of phosphor coatings of different thicknesses, fabricated based on phosphors of different types.

Table 2. Results of measuring the colour- and photometric characteristics of phosphor samples.

Sample	x	y	CCT/K	CRI	Φ_v/lm
1	0.2801	0.2773	7732	61	78.3
2	0.3115	0.3302	7000	62	92.4
3	0.4254	0.5105	3572	62	85.1
4	0.2899	0.2812	7352	65	135.3
5	0.3303	0.3487	5595	66	165
6	0.4075	0.4751	3950	64	142.8
7	0.2925	0.2875	7202	63	99.2
8	0.3415	0.3575	4172	64	128
9	0.3954	0.4495	3874	64	108.3

Figure 2 shows the experimental values of colour coordinates x and y for the samples under study. It can be seen that the colour coordinates for samples 1, 4, and 7, which had a phosphor-layer thickness $h_1 = 0.6$ mm, corresponded to ‘cold’ white light with a CCT value above 6600 K. This can be explained by the fact that phosphor coating film was very thin. Hence, as a result of the superposition of the laser light transmitted through the phosphor layer without absorption and the radiation spontaneously emitted by the phosphor, the spectrum of the resulting radiation had a stronger blue component. This is evidenced by the spectrum of the resulting radiation from sample 1 (see Fig. 3a).

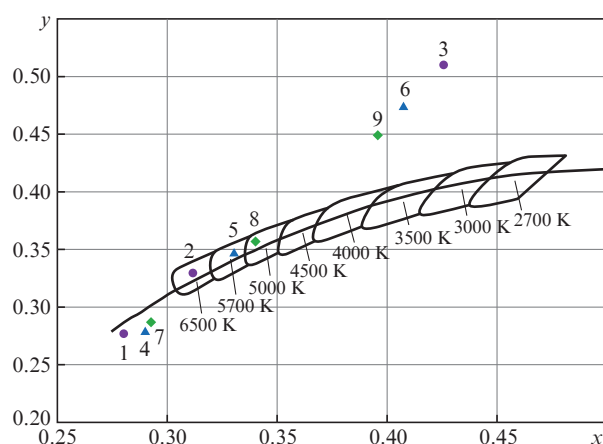


Figure 2. Experimental values of colour coordinates x and y for samples 1–9 (symbols) and tabular values of colour coordinates of absolutely black body (solid line), with selected areas of white light colour coordinates corresponding to different CCTs.

One can see two spectral maxima in Fig. 3a. The first lies in the short-wavelength region (in the range of 443–445 nm) and corresponds to the spectrum of the laser radiation source, while the second (a longer wavelength one), is located in the yellow-green spectral region and corresponds to the luminescence spectrum of the phosphor based on $\text{YAG}:\text{Ce}^{3+}$.

The intensity of the band corresponding to the phosphor luminescence in the spectrum of sample 9 (Fig. 3b) greatly exceeds that in the spectrum of sample 1 (Fig. 3a). Samples 3 and 6 exhibited similar spectral characteristics. The thickness h_3 of the deposited phosphor coating for samples 3, 6, and 9 was the same: 1.4 mm. This change in the intensity ratio for the blue and yellow-green components is related to the larger thickness of the phosphor coating, which results in higher absorption of laser radiation in comparison with the samples with the coating thickness $h_1 = 0.6$ mm. The colour coordinates for samples 3, 6, and 9 lie in the yellow region; the CCT value was found to be 3000–3500 K.

Samples 2, 5, and 8 with a phosphor-layer thickness $h_2 = 1$ mm had colour characteristics similar to those of blackbody radiation, with CCT values of 6500, 5700, and 5000 K, respectively. The spectrum of the resulting radiation from sample 5 is presented in Fig. 3c.

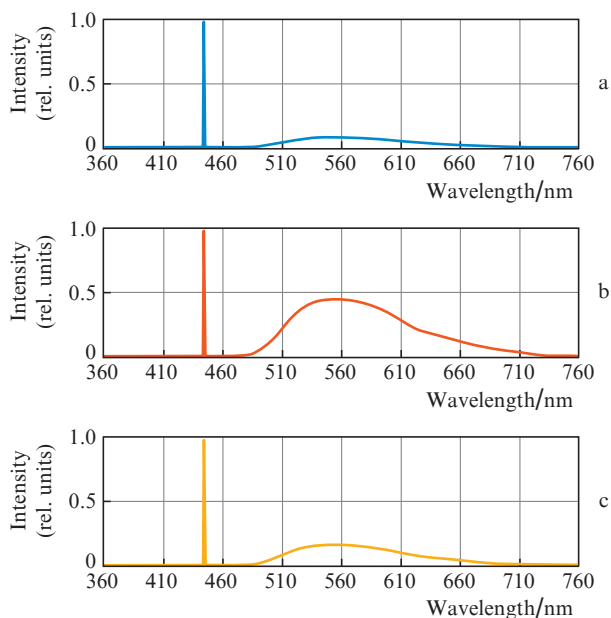


Figure 3. Spectra of samples (a) 1, (b) 9, and (c) 5.

Then we investigated the dependences of the colour coordinates and photometric characteristics of samples 2, 5, and 8 on the output power of the laser module. Figure 4 shows the dependences of measured colour coordinates x and y on the output power P_{out} . It can be seen that colour coordinates decrease with an increase in P_{out} . This behaviour can be explained by the fact that a rise in output power increases the amount of heat released in the phosphor layer due to the Stokes effect. As a result, the phosphor luminescence intensity drops, and the resulting radiation spectrum changes.

Figure 5 shows dependences of CCT on the output power P_{out} . One can see a slight (within 100 K) increase in CCT with an increase in P_{out} from 0.01 to 1 W for samples 5 and 8. For sample 2, the CCT values increase from 5450 to 5700 K under these conditions. The change in the colour coordinates and CCT value for sample 2 is indicative of a fluctuation of the spectral composition of the resulting radiation with an increase in P_{out} . This fluctuation may be related to the grain size inhomogeneity in powder phosphor FLZh-7-560. As a result, smaller grains are heated more rapidly and strongly than larger

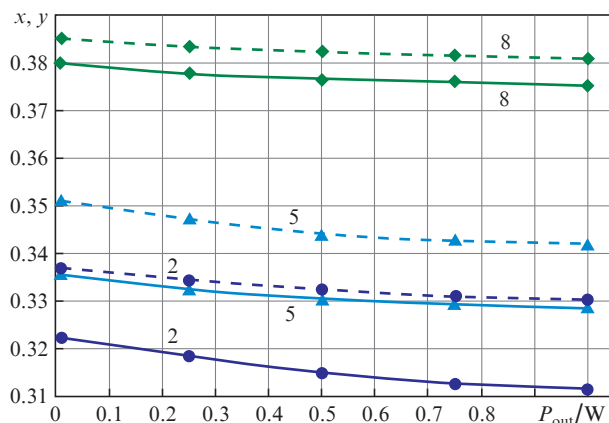


Figure 4. Dependences of the colour coordinates (solid lines) x and (dashed lines) y on the output power P_{out} for samples 2, 5, and 8.

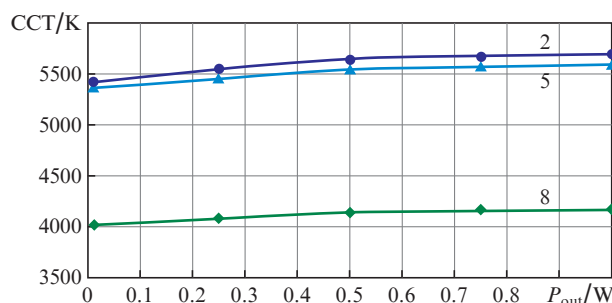


Figure 5. Dependences of CCT on the output power P_{out} for samples 2, 5, and 8.

ones due to the Stokes effect. Heat release enhances the influence of nonradiative recombination processes, which causes even stronger heating. A positive feedback arises, and the internal and external quantum efficiencies of the phosphor decrease.

Another possible factor is the inhomogeneity of the phosphor composition. It is known that three compounds can be formed in the $Y_2O_3-Al_2O_3$ system: $YAlO_3$ (YAP), $Y_2Al_5O_3$ (YAG), and $Y_4Al_2O_{12}$ (YAM). Cooling of the $Y_2O_3-Al_2O_3$ melt [16–18] may cause (along with the formation of garnet) metastable crystallisation of the eutectic melt. In addition, it was suggested in [19] that the dopant (cerium) in YAG single crystal may exist in both the Ce^{3+} and Ce^{4+} states. The absorption band of $YAG:Ce^{3+}$ coincides with that of $YAG:Ce^{4+}$; however, the recombination is nonradiative. This effect leads to a decrease in the resulting luminous flux due to the decrease in the blue component intensity in its spectrum and causes simultaneously additional heating of the phosphor.

Figure 6 shows dependences of CRI on the output power P_{out} of the laser module. The maximum CRI value is 67 for sample 5; however, it decreased to 66 with an increase in P_{out} . The minimum CRI value is 62 for sample 2.

The small CRI value (smaller than 75) for all samples can be explained by the absence of emission in the spectral ranges of 360–442 nm and 445–475 nm and low intensity of spontaneous phosphor emission in the red (650–780 nm) spectral region.

Figure 7 shows the lumen–current characteristics of the samples studied. It can be seen that the luminous flux does

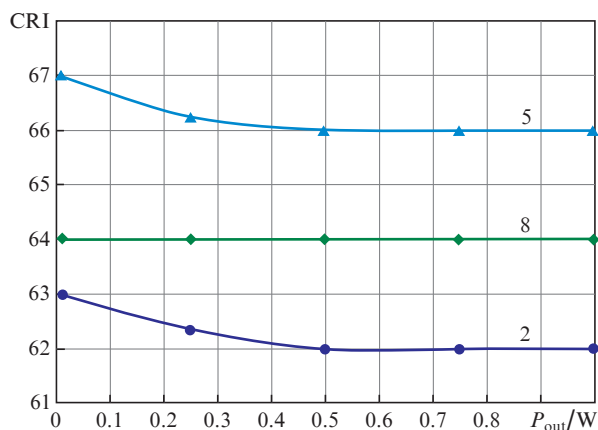


Figure 6. Dependences of CRI on the output power P_{out} for samples 2, 5, and 8.

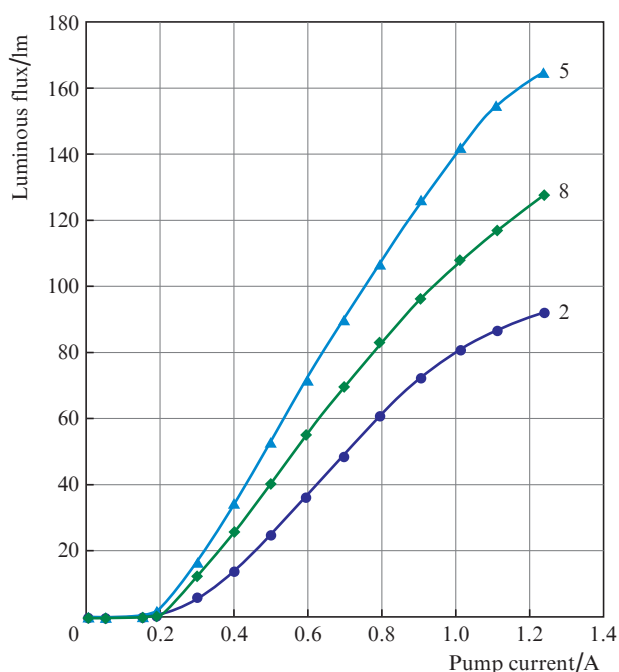


Figure 7. Lumen-current characteristics of samples 2, 5, and 8.

not rise with an increase in the pump current in the initial stage; this fact indicates the absence of laser diode lasing. When the pump current exceeds the threshold value (0.2 A), the luminous flux starts increasing with the pump current; however, this dependence is nonlinear. This can be explained by the presence of nonradiative recombination. When the pump current exceeds 0.4 A, the lumen-current characteristic becomes linear, and the luminous flux tends to a constant value after the pump current reaches 0.9 A.

Figure 8 shows the dependences of the light efficacy of the samples on the consumed electric power. It can be seen that in the initial portion (near the lasing threshold of the laser diode), at low output power, the light efficacy linearly increases with an increase in the consumed electric power. With a further rise in the consumed power, the light efficacy continues increasing, reaches a maximum, and then begins to decrease. The maximum value of the light efficacy was 30 lm W^{-1} at a consumed electric power of 4.2 W for sample 5, which corresponds to a pump current of 1.24 A. This value of the

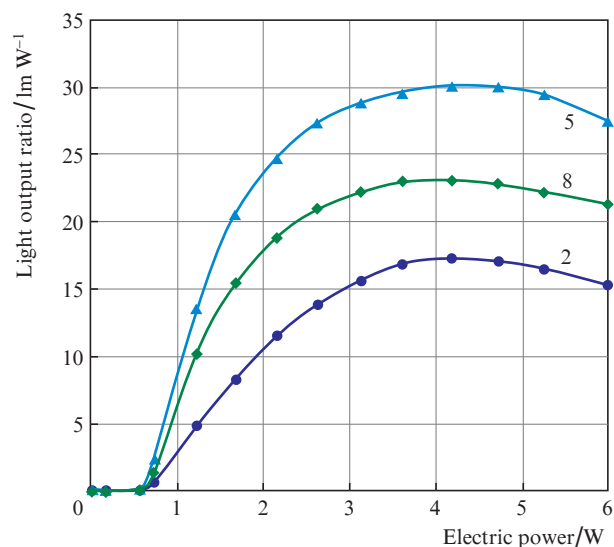


Figure 8. Dependences of the light efficacy on consumed electric power for samples 2, 5, and 8.

light efficacy significantly exceeds the incandescent lamp efficiency and is comparable with the corresponding parameter of commercial white LED sources.

The saturation of the characteristics presented in Figs. 7 and 8 can be explained by the combined effect of the following factors:

(i) decrease in the laser beam coupling coefficient into the optical fibre because of the increase in the beam divergence in the far field (in the plane parallel to the p-n junction) with an increase in the laser diode pump current;

(ii) phosphor heating under laser irradiation.

Based on the above-said, we can suggest that, when developing laser illumination systems, the conventional technologies used to fabricate illuminating devices based on blue LEDs (specifically, the use a mixture of phosphor powder and transparent compound) may be of little use. Laser illumination systems based on cerium-doped yttrium aluminium garnet single crystals or luminescent ceramics ($\text{YAG}:\text{Ce}^{3+}$) can be considered as the most promising ones. Since the thermal conductivity of single crystals or ceramics based on $\text{YAG}:\text{Ce}^{3+}$ exceeds that of a phosphor powder placed in a compound, the photometric characteristics of these illuminating devices may exceed those reported in this paper.

4. Conclusions

We investigated the possibility of applying the classical technology of fabricating phosphor coatings to design lighting systems with excitation of phosphor luminescence by the laser light.

It was shown that, when implementing a lighting system based on excitation of phosphor luminescence by laser radiation, the conventional technologies used for fabricate lighting systems based on white LEDs may be of little use.

The main photometric characteristics (colour coordinates, CCT, and CRI) of phosphor coatings based on $\text{YAG}:\text{Ce}^{3+}$ powder from different Russian manufacturers were investigated.

Excitation of phosphor luminescence by laser radiation from a fibre-optic module with an output power of 1 W, operating in the cw regime and emitting at $\lambda = 445 \pm 3 \text{ nm}$, provided

the following characteristics: maximum luminous flux of 165 lm, colour coordinates $x = 0.3303$ and $y = 0.3487$ (CIE 1931), correlated colour temperature of 5595 K, colour rendering index of 66, and light efficacy of 30 lm W^{-1} .

The obtained characteristics of the white light source based on excitation of phosphor luminescence by laser radiation are close to those of commercial white LED lighting systems.

References

1. Schubert E.F. *Light-Emitting Diodes* (Cambridge: Cambridge Univ. Press, 2006).
2. Rozhansky I.V., Zakheim D.A. *Phys. Status Solidi C*, **3**, 2160 (2006).
3. Kim M.H., Schubert M.F., Dai Q., Kim J.K., Schubert E.F., Piprek J., Park Y. *Appl. Phys. Lett.*, **91**, 183507 (2007).
4. Shen Y.C., Mueller G.O., Watanabe S., Gardner N.F., Munkholm A., Krames M.R. *Appl. Phys. Lett.*, **91**, 141101 (2007).
5. Efremov A.A., Bochkareva N.I., Gorbunov R.I., Larinovich D.A., Rebane Y.T., Tarkhin D.V., Shreter Y.G. *Semiconductors*, **40**, 605 (2006).
6. Chichibu S., Azuhata T., Sota T., Nakamura S. *Appl. Phys. Lett.*, **69**, 4188 (1996).
7. Nakamura S. *Science*, **281**, 956 (1998).
8. Xu Y., Chen L., Li Y., Song G., Wang Y., Zhuang W., Long Z. *Appl. Phys. Lett.*, **92**, 021129 (2008).
9. Ryu H.-Y., Kim D.-H. *J. Opt. Soc. Korea*, **14** (4), 415 (2010).
10. Kristin A.D., Cantore M., Nakamura S., DenBaars S.P., Seshardi R. *AIP Advances*, **3**, 072107 (2013).
11. Wierer J.J. Jr, Jeffery Y., Tsao J.Y., Sizov D.S. *Laser Photonics Rev.*, **7**, 963 (2013).
12. Ledru G., Catalano C., Dupuis P., Zissis G. *AIP Advances*, **3**, 107134 (2014).
13. Abdullaev O.R., Akhmerov Yu.L., Mezheny M.V., Chelny A.A. RF Patent No. 165548, *Byull. Izobret. Poleznykh Modelei*, No. 29 (2016).
14. Akhmerov Yu.L., Ivanov A.A., Flider P.S., Chelny A.A. RF Patent No. 168128, *Byull. Izobret. Poleznykh Modelei*, No. 2 (2017).
15. Akhmerov Yu.L., Ivanov A.A., Flider P.S., Chelny A.A. RF Patent No. 169744, *Byull. Izobret. Poleznykh Modelei*, No. 10 (2017).
16. Cokayne B., Lent B. *J. Cryst. Growth*, **46**, 371 (1974).
17. Caslavsky J.L., Viechnicki D.J. *J. Mater. Sci.*, **15** (7), 1709 (1980).
18. Briskina Ch.M., Rumyantsev S.I., Ryzhkov M.V., Soshchin N.P., Spasskii D.A. *Svetotekhnika*, **5**, 37 (2012).
19. Wang L., Zhuang L., Xin H., Huang Y., Wang D. *Open Inorg. Chem. J.*, **5**, 12 (2015).